Experimental Studies of Alfvén Mode Stability in the JET Tokamak

D.Testa[1], A.Fasoli[1,2], R.Bertizzolo[1], D.Borba[3], R.Chavan[1], S.Huntley[4], V.Riccardo[4], S.Sanders[4], J.A.Snipes[2], P.Titus[2], R.Walton[4], M.Way[4], JET-EFDA contributors[*]

[1] CRPP, Association EURATOM – Confédération Suisse, EPFL, Lausanne, Switzerland
[2] Plasma Science and Fusion Center, Massachusetts Institute of Technology, Boston, USA
[3] Associacão EURATOM/IST, Av. Rovisco Pais, 1049-001 Lisboa, Portugal
[4] EURATOM-UKAEA Fusion Association, Culham Science Centre, OX14 3DB, Abingdon
E-mail of main author: duccio.testa@epfl.ch)

1. Introduction

Controlling the interaction between fusion generated α's and modes in the Alfvén frequency range is a crucial issue for the operation of experimental reactors in the burning plasma regime, such as ITER, as these modes can be driven unstable by the slowing-down α's up to amplitudes at which they could cause rapid radial transport of the α's themselves. The need to avoid strongly unstable regimes for some classes of Alfvén Eigenmodes (AEs) could therefore provide additional operational limits for the reactor regime. On the other hand, if adequate actuators are identified, AEs could be used to affect the thermonuclear plasma burn in a controlled way.

Two classes of investigations are conducted on JET to directly observe the AE stability limits in the presence of fast particles that can resonate with the modes and to measure the damping rate of the modes as a function of the plasma parameters, in order to quantify the mechanisms that provide background damping for the modes in different conditions. Sections 2 and 3 describe experiments from the first class, addressing the AE stability threshold for different fast ion radial distributions, generated at different locations by additional heating or at different plasma densities, or modified by the presence of error field mode. Examples from the second class are described in Section 4. During the last two years a particular effort was undertaken to complete the database of damping rate measurements of low toroidal mode numbers using the saddle coil active AE excitation system, which is being dismantled during the 2004 JET shutdown. A new antenna system is under development to continue along the same lines, but extending the accessible range of toroidal mode numbers to higher values, up to n≈10-15, of more direct relevance to ITER. This system is described in Section 5.

2. Effect of the ICRF heating scheme and of plasma density on the AE stability threshold

Different Ion Cyclotron Resonance Frequency (ICRF) heating schemes are used to create different distributions of energetic particles, with energies in the MeV range, and test their stability with respect to AEs. As a first example, a simple method to affect the radial distribution of fast ions is to change the difference in frequency between independent ICRF modules. A broad fast ion pressure profile can be produced by operating the four JET ICRF antennas at four different frequencies. A wider ICRF power deposition profile corresponds to a lower fast ion pressure gradient, $\nabla\beta_{FAST}$, in the plasma core, thus leading to a reduced mode activity in the Alfvén frequency range [1].

Here we assess the difference on the fast ion distribution function $f_{FAST}(E,r)$ and the perpendicular temperature $T_{\perp FAST}(r)$ between single-frequency (monochromatic) and multi-frequency (polychromatic) minority hydrogen H(D) ICRF heating for similar background plasma parameters, and the effects of such differences on the spectra of fast ion driven AE instabilities. Multi-frequency ICRF heating gives rise to a lower $T_{\perp FAST}$ in the plasma core, as

[*] See annex 1 of J.Pamela et al., "*Overview of Recent JET Results*", OV-1/1.4, Fusion energy 2002 (Proc. 19th International Conference, Lyon, 2002) IAEA, Nuclear Fusion 43 (2003), 1540.

measured with a high energy NPA [2]. Earlier measurements of $f_{FAST}(E,r)$ have also shown that, for the same level of P_{ICRF}, polychromatic heating gives rise to a broader $T_{FAST}(r)$, to a more peaked electron temperature profile $T_e(r)$, and to an increase in the central ion temperature T_{i0}, or to the same T_{i0} for a much higher central electron density n_{e0} [3]. This may have favourable implications for ITER operation since the lower $T_{\perp FAST}$ approaches the critical temperature at which fast ions preferentially heat the fuel ions through collisions, but the reduced collisional heating on the electrons, reducing the electron temperature, may in turn adversely affect the current drive efficiency.

To confirm these initial results in a more systematic way, we have compared discharges with the same P_{ICRF} and very similar electron density profiles. For the case of polychromatic heating we observe high-n Toroidal AEs located at the q=2 surface and high-n Ellipticity-induced AEs located at the q=3 surface, closer to the plasma edge. Conversely, for the case of monochromatic heating we only observe q=2 TAEs with significantly higher amplitude, but no EAEs. The presence/absence of the q=3 EAEs and the lower amplitude of the q=2 TAEs confirms that $f_{FAST}(E,r)$ has a broader radial profile, less peaked on-axis, for polychromatic than for monochromatic heating. This suggests a more extensive use of the polychromatic heating scheme in JET for further scenario improvements, also in view of ITER operation.

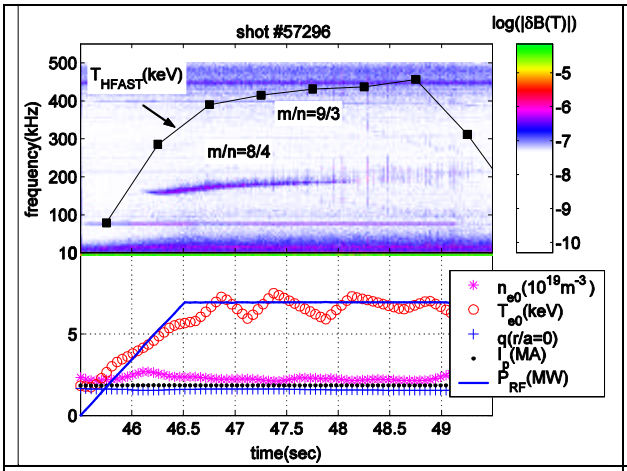

Figure 1a. Mode activity in the Alfvén frequency range for the case of polychromatic ICRF heating. Here only weak TAEs and EAEs are observed.

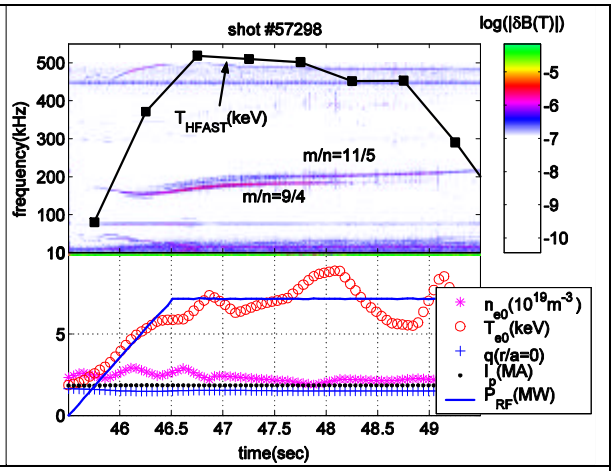

Figure 1b. Mode activity in the Alfvén frequency range for the case of monochromatic ICRF heating. Here strong core localised TAEs are observed.

Operation at high density is beneficial for the burning plasma regimes in ITER. The DT fusion cross section has a broad peak around $E_D \approx E_T \approx 70$keV/amu, and the temperature of the bulk plasma ions has to reach comparable values in order to maximise the fusion yield. The use of 2nd harmonic minority ICRF heating at higher plasma density reduces $T_{\perp FAST}$ in the plasma core due to the lower energy at which the RF diffusion coefficient goes to zero [4], but gives rise to a lower fast ion driven plasma rotation [1]. The reduced rotation may in turn negatively affect the stability of current and pressure driven modes, and limit the possibilities to control turbulence and the transition to high confinement regimes through sheared flow generation [5]. In view of possible extrapolations of the minority ICRF heating schemes used in JET to the heating of the fuel ions in ITER, it is then important to study the stability of fast ion driven AEs as a function of the plasma density for otherwise similar plasma conditions.

First, the most obvious effect of plasma density on ICRF-driven fast ions comes from the dependency of the fast ion slowing down time, $\tau_S \sim T_e^{3/2}/n_e$. Second, the RF diffusion coefficient goes to zero at lower fast ion energy for increasing plasma density due to the larger perpendicular wave number of the ICRF wave field, effectively preventing a formation of a tail in $f_{FAST}(E)$ above a certain energy. This critical energy decreases with the harmonic number, from >3Mev for 1st harmonic heating to ≤1MeV for 2nd and higher order harmonic.

To test this theoretical result and benchmark ICRF code calculations, a series of experiments were performed using the 2nd harmonic H(D) ICRF heating scheme. The ICRF power, P_{ICRF}=5.2MW, the electron temperature profile and the shape of the electron density profile were the same for the various discharges, thus allowing for a direct comparison of T_{FAST} as function of the electron density in the plasma core n_{e0}. The measured $T_{\perp FAST}$ is almost double at low plasma density, $T_{\perp FAST}\approx$200keV at $n_{e0}\approx3\times10^{19}m^{-3}$ compared to $T_{\perp FAST}\approx$120keV at $n_{e0}\approx4\times10^{19}m^{-3}$. Correspondingly, much weaker q=2 TAEs are excited for similar values of P_{ICRF}, thus indicating a much lower drive at the mode radial location, as shown in fig.2. These results are in quantitative agreement with current modelling of the various ICRF heating schemes [4], with encouraging prospects for predictions of ICRF scenarios in ITER.

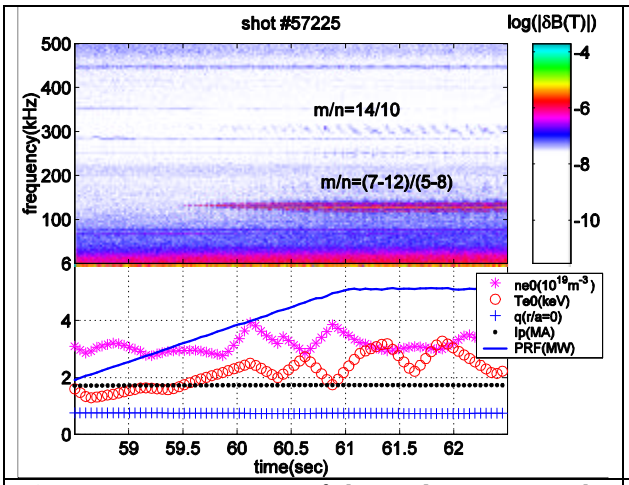

Figure 2a. Measurement of the mode activity in the Alfvén frequency range for the case of lower plasma density, $n_{e0}\approx3\times10^{19}m^{-3}$, thus higher $T_{\perp FAST}\approx$200keV.

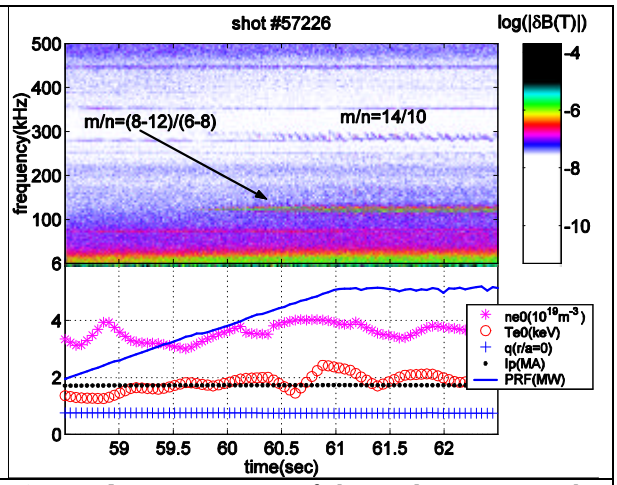

Figure 2b. Measurement of the mode activity in the Alfvén frequency range for the case of higher plasma density, $n_{e0}\approx4\times10^{19}m^{-3}$, thus lower $T_{\perp FAST}\approx$120keV.

3. Effect of error fields on the stability threshold of ICRH driven AEs

The AE stability can be affected by the onset of other instabilities that modify the AE drive by causing a redistribution of the fast ions. Two examples, already described in [6], are the rapid density perturbation associated with pellet injection and the appearance of a q=1 magnetic island associated with a sawtooth crash. To further these earlier studies, we investigated the effect on the fast particle population, hence the AE drive, of externally induced error fields locking to the q=2 surface and generating a magnetic island. The interest for this kind of experiment stems from the fact that an ad-hoc radial redistribution of the fast ions could in principle be beneficial in locally reducing $\nabla\beta_{FAST}$, hence the drive for AEs or Energetic Particle Modes.

In the absence of radially resolved measurements of $f_{FAST}(E,r,t)$, the onset and the disappearance of AEs localised at different radial positions can be used to provide evidence for fast ion redistribution. In these experiments, the in-vessel saddle coils were used in their low-frequency mode of operation to apply an externally controlled error field around the q=2 surface. With and without such error field, we observe EAEs associated with the q=3 surface, whereas with the error fields we do not observe q=2 TAEs, as we do without the error fields. This indicates that the net drive for these modes has been lowered by the error fields and the induced magnetic island around the q=2 surface, with a much weaker effect around the q=3 surface [1].

Similarly, without the error fields, n=4 TAEs become unstable at $P_{ICRF}\approx$3MW, and during the ICRF flat-top phase reach the amplitude at the plasma edge $|\delta B|_{TAE}\approx1.3\times10^{-5}$T. The only difference observed for the n=4 EAE when the error fields are applied is the much higher excitation threshold, $P_{ICRF}\approx$1.1MW without error fields compared to $P_{ICRF}\approx$2MW with error

fields, thus indicating that a larger drive is required in this case. The slightly different central electron temperature, T_{e0}<3keV without error fields compared to T_{e0}~4keV with error fields, does not affect significantly the TAE stability but gives a further indication that the fast ion temperature is larger in the plasma core without error field modes. These observations can be interpreted by considering that the presence of a magnetic island causes a radial redistribution of the fast ions. The detailed modelling of these experimental results is left for future work.

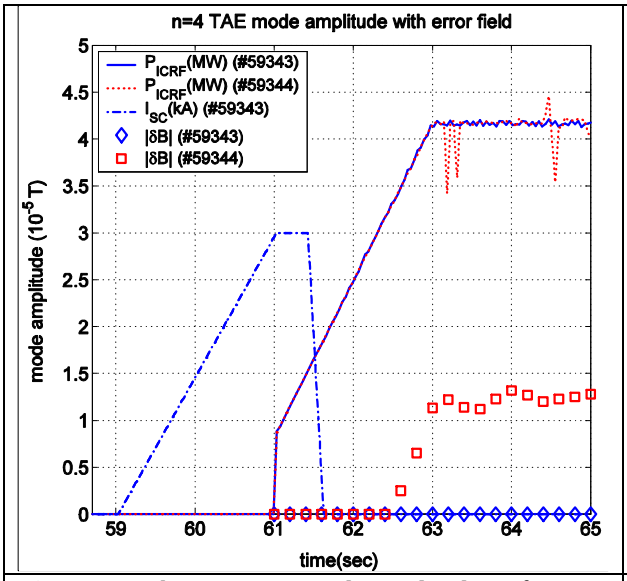

Figure 3a. The n=4 TAE mode amplitude as function of P_{ICRF}. No mode is observed with error fields, and it becomes unstable at P_{ICRF}≈3MW without error fields.

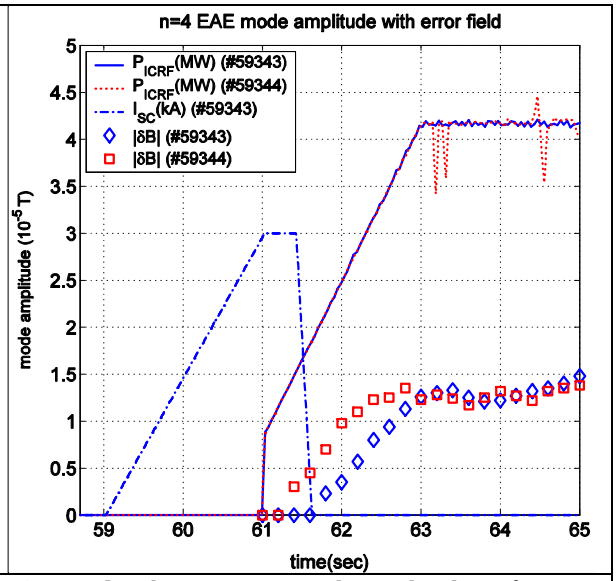

Figure 3b. The n=4 EAE mode amplitude as function of P_{ICRF}. The P_{ICRF} excitation threshold is higher with, P_{ICRF}≈2MW, that without error fields, P_{ICRF}≈1.1MW.

4. Effect of the value of the safety factor on axis, of the plasma rotation and its shear, and of the direction of the ion ÑB-drift on the damping rate for n=1 TAEs

One of the main purposes of the AEs studies on JET is to validate the existing theoretical models and identify the dominant damping mechanisms for global AEs, with the aim to improve the accuracy in the predictions for future burning plasma experiments such as ITER. This approach has characterised the AE active excitation experiments in JET over the last ten years, using the saddle coils as an AE active antenna. The last campaigns aimed at completing the saddle coil database before their removal, in the second half of 2004.

Along this line, we have investigated the role of the central safety factor q_0, of the plasma rotation and of the direction of the ion ∇B-drift on the AE stability in plasmas with a monotonic q-profile. Due to the strong increase of the damping rate for the saddle coil driven, low-n AEs at high edge elongation (κ_{95}>1.6) and triangularity (δ_{95}>0.35) [7], which makes it difficult to measure low-n AEs in such configurations, our experimental work has mainly focused on plasmas with low κ_{95} and δ_{95}, so as to infer in detail the contribution of additional damping mechanisms in regimes much closer to the marginal stability limit of low-n AEs.

Theoretical modelling and direct measurements indicate that low-n AEs have a global structure, i.e., have a radial profile extending over a large fraction of the plasma cross-section. The rotation f_{ROT} of the whole plasma column, and the shear in it $(r/f_{ROT})(df_{ROT}/dr)$, can thus be expected to have an impact over the effective mode damping. Comparing discharges with similar level of Neutral Beam power (P_{NBI}), we notice that for P_{NBI}≤5MW the shear in the plasma rotation has no clear effect on the damping rate of n=1 TAEs. Only for P_{NBI}>6.5MW a general trend can be identified in the database we collected, namely that the damping rate for n=1 TAEs is always γ/ω>2% in discharges characterised by a higher rotation shear, as shown in figs.4a and 4b. This suggests that the damping mechanisms active at low performance are

different from those active at high performance, with the former not affected by the toroidal rotation profile of the plasma column and its shear.

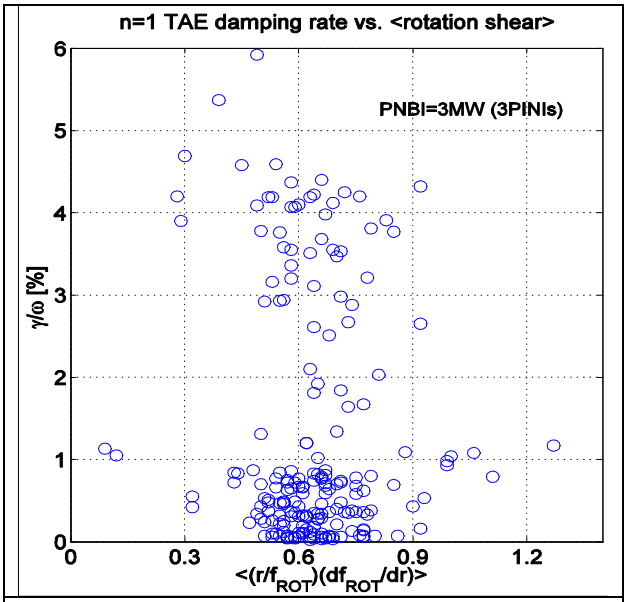

Figure 4a. Damping rate for n=1 TAEs as function of the volume-averaged rotation shear for P_{NBI}=3MW: note the large scatter in the values of γ/ω.

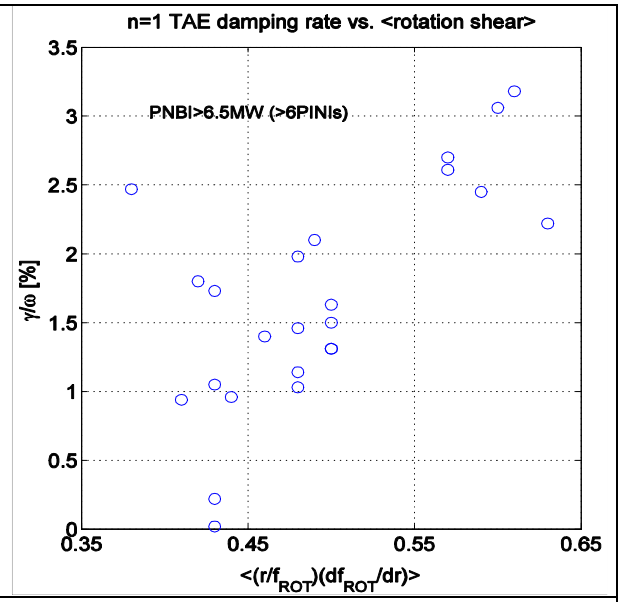

Figure 4b. Damping rate for n=1 TAEs as function of the volume-averaged rotation shear for P_{NBI}>6.5MW: here for high rotation shear γ/ω>2% always.

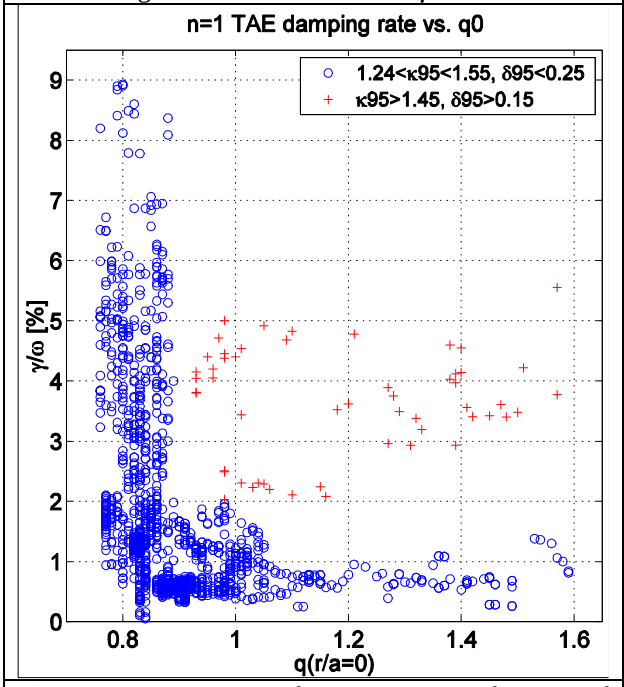

Figure 5. Damping rate for n=1 TAEs as function of q_0 in ohmic plasmas: we note that for q_0>1.1 a large γ/ω>2% is obtained only for κ_{95}>1.45 and δ_{95}>0.15.

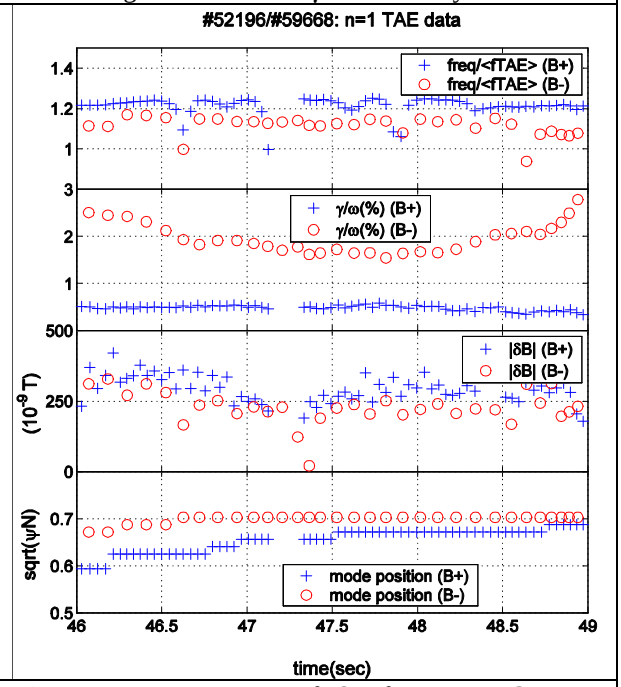

Figure 6. Measurement of the frequency, damping rate, mode amplitude and radial position for n=1 TAEs as function of the ion ∇B-drift direction.

Considering ohmic plasmas with κ_{95}<1.5 and δ_{95}<0.3, we find that for q_0>1.1 the damping rate of n=1 TAEs does not exceed the value $\gamma/\omega\approx$2% for a variety of electron density and temperature profiles and for different values of the plasma current and magnetic field, as shown in fig.5. Conversely, with q_0<0.9, we find that in the same experimental conditions γ/ω can reach values up to $\gamma/\omega\approx$8%. These observations indicate that very large values of the damping rate (γ/ω>2%) can only be obtained for q_0<1. Theoretical modelling is necessary to reproduce and provide an interpretation for this phenomenon. The transition between these two regimes, which is observed for $q_0\approx$0.9-1.1 is suggestive of a role for the sawteeth, either a

dynamical one associated to each individual sawtooth collapse, or an average effect of the sawteeth redistribution providing, on average, a lower core shear, favouring core damping via mode conversion [8].

The direction of the ion ∇B-drift is an important parameter in determining the accessibility conditions for the H-mode regime, with multi-machine experimental evidence that a lower additional heating power is required for the L-H mode transition when the ion ∇B-drift is directed towards the divertor [9]. It is thus important to study the implications of the choice on the ion ∇B-drift direction foreseen for ITER operation on the value of the background plasma damping of low-n TAEs. The data shown in fig.6 indicate that the damping rate of n=1 TAEs with similar frequency and radial location is approximately a factor three higher for the case of ion ∇B-drift directed away from the divertor, suggesting that low-n TAEs would have a much lower instability threshold in plasma configuration with the ion ∇B-drift directed towards the divertor [1].

After about ten years of operation, the 2004 JET experimental campaigns have been the last where the saddle coils have been used to drive and detect the damping rate of low-n TAEs. This experimental work has been useful in providing detailed benchmarks for the theoretical predictions of the TAE stability in ITER, see for instance Refs.[7,8,10,11]. In particular, we have demonstrated the role of the edge elongation, triangularity and magnetic shear in determining γ/ω for low-n TAEs [7], and we have measured the dependence of the damping rate on the bulk plasma beta [10] and normalised Larmor radius [11]. In this respect, the measurements reported here of the dependence of γ/ω for n=1 TAEs on the rotation shear, safety factor on axis and direction of the ion ∇B-drift represent the logic conclusion of our experimental effort on low-n TAEs. On the theoretical side, we have learnt that gyrokinetic codes provide for a better understanding of the damping rate of low-n TAEs, and particularly the dynamic scaling of γ/ω as function of various plasma parameters such as the edge plasma shape, the bulk plasma beta and the normalised ion Larmor radius, see for instance the results presented in Refs.[8,11]. However, it is also clear that a more systematic effort is needed for accurate predictions of TAE instabilities in ITER, and this work should start from the large database of low-n TAE data that we have collected so far, of which the data presented in this paper are a typical example. At the same time, the design and installation of the new high-n TAE antennas for JET represent the logic step forward towards a more detailed benchmarking of the existing models for high-n AEs in ITER regimes.

5. Outlook: the new JET antenna for the excitation of high-n AEs

The present antenna geometry limits the active AE excitation to low toroidal mode numbers, n=0-2, whereas intermediate or high n's characterise the most unstable AEs, which are already detected in JET and are similarly predicted for ITER. A direct excitation and tracking of the same modes is thus of clear interest for preparing the next step experiment. To this end, an antenna structure optimised for the excitation and detection of AEs with $n\approx10$-15 has been designed and built, and it is being installed during the current JET shutdown [12].

The new antenna system comprises two assemblies of 4 toroidally spaced coils, situated at opposite toroidal locations. The static self-inductance of each new coil is $L\approx25\mu H$, similar to that of the old antennas. Each coil is made using 18 turns of 4mm Inconel 718 wire, covers an extent of ~(25×25×15)cm, and is individually insulated from the supporting frame with Alumina-Oxide spacers. The first turn sits ~45mm behind the poloidal limiters. The coils are mounted on a 3mm-thick Inconel 625 open structure, to avoid a closed path for disruption-induced currents. A sketch of one set of four coils is shown in fig.7a. Figure 7b illustrates the integration of one set of four coils into the JET first wall.

The support scheme uses cantilevered brackets that connect to the remains of the saddle coils and “wing” brackets which add support to the top of the frame. These four attachment points are isolated with Shapal-M spacers and bypassed with straps of known resistance to provide a reliable current path, and hence optimise the mechanical load distribution. The frame is further protected by CFC tiles. Conservative estimates of the disruption currents in the MHD antennas and frame were used to calculate the loading and resulting stress in the antenna structure. The frame is designed as an open structure to break eddy current loops, computed assuming the antenna is shorted. The forces on the frame primarily result from halo currents entering around the mini limiters that now protect the coils. Initially, halo current loads were calculated assuming the full inventory of halo current crossed the toroidal field and passed downward the full height of the frame to the lower attachment points. This caused excessive forces at the saddle coil attachment points. To improve the loading, the attachment points were connected to their mounting locations through resistive straps which have their resistances sized to produce currents that minimise the net loading. With the addition of the resistive earth straps at the four attachment points, a small toroidal current crossed with the poloidal field component is added but the much larger loading due to poloidal currents crossed with toroidal field is hugely reduced. Figure 7c shows an example of the calculation of the mechanical loads and stresses in the antenna structure, due to halo currents during plasma disruptions, and, to a lesser extent, to disruption induced currents, in both cases crossed with the ambient magnetic field. Figure 7d shows a photo of the antenna frame, ready for the final coil assembly.

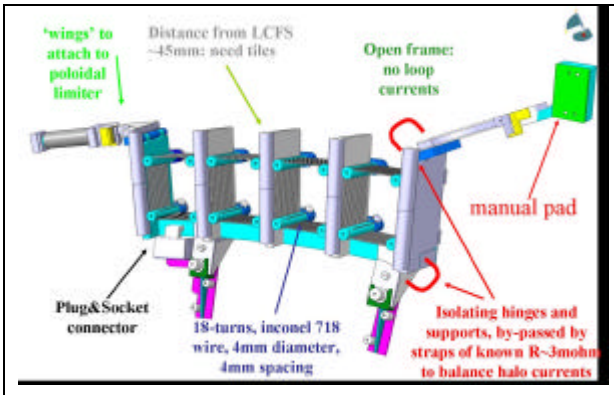

Figure 7a. Final design of the new TAE antennas.

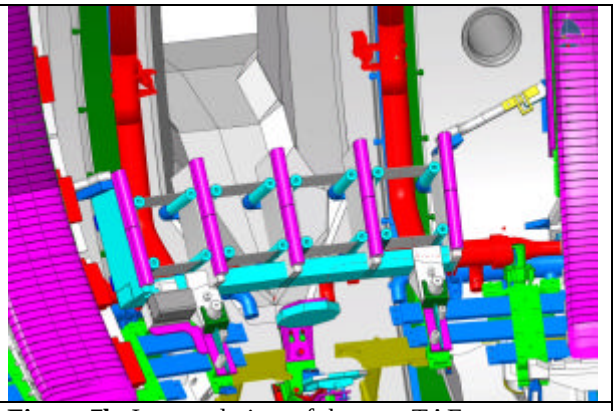

Figure 7b. In-vessel view of the new TAE antennas.

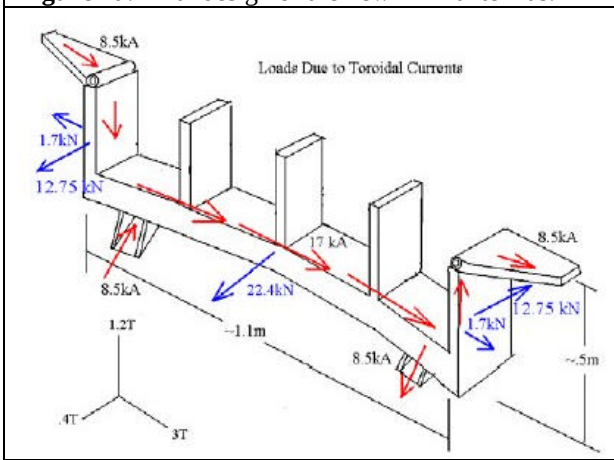

Figure 7c. Stress analysis of the new TAE antennas.

Figure 7d. One of the two antenna frames as built.

To comply with the “As Low As Reasonable Possible” system for manual in-vessel access, the new antennas will be almost entirely installed by Remote Handling (RH). Hence many components and jigs had to be specially designed to be compliant with the requirements of the RH installation. Detailed engineering work, the adaptable JET RH capabilities and

virtual reality models were used to develop the installation procedure. This has been recently successfully demonstrated in full mock-up trials, thus significantly reducing the engineering risks associated with the actual in-vessel installation.

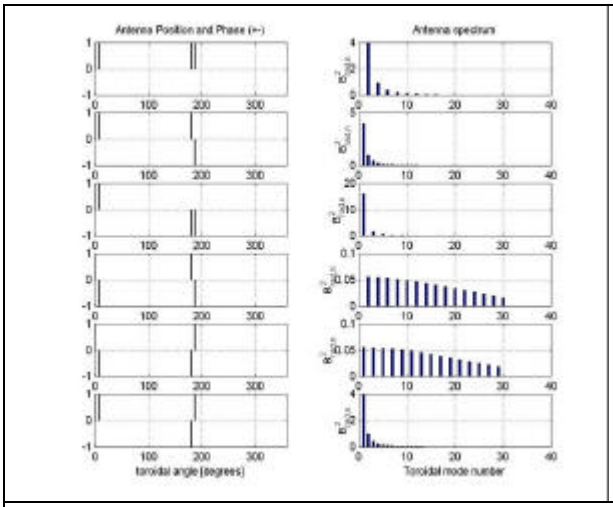

Figure 8a. Excited spectrum using 4 opposite coils.

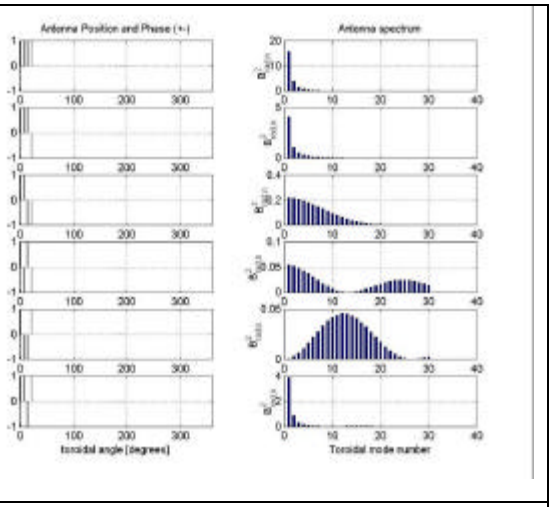

Figure 8b. Excited spectrum using 4 adjacent coils.

To simplify the ex-vessel installation, only four out of the eight antennas will be actively driven, and the four "passive" ones will be used as additional detectors, together with magnetic pick-up coils and internal measurements such as ECE and reflectometry. The maximum antenna current and voltage used for the AE excitation experiments are of the order of 10A and 700V, producing a very small antenna-driven magnetic field, $|dB/B|<10^{-5}$. Any combination of 4 out of the 8 antennas will be chosen to excite different n-spectra, up to n~20, as shown in fig.8a and fig.8b.

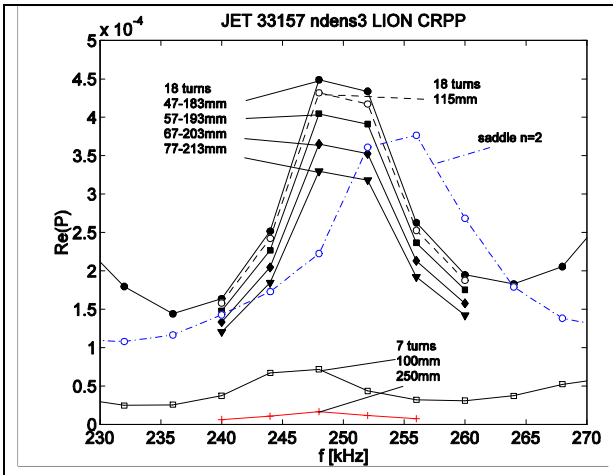

Code calculations also demonstrate that this arrangement provides a coupling to the plasma for a n=5 TAEs that is of the same order as that achieved with the present, much bigger, saddle coils for an n=2 TAE for the same JET equilibrium, as shown in fig.9. Thus, it is foreseen that the real-time tracking capabilities of the old saddle coil system will be maintained and, possibly, control of the marginal stability limit could be envisaged for the intermediate n-modes driven by the new antennas.

Figure 9. Calculated coupling for new TAE antennas.

This work has been conducted under the European Fusion Development Agreement. D.Testa and A.Fasoli were partly supported by the Fond National Suisse pour la Recherche Scientifique, Grant 620-062924. A.Fasoli, J.A.Snipes and P.Titus were partly supported by the US DoE Contract DE-FG02-99ER54563.

References

[1] D.Testa et al., PPCF **46** (2004), S59. [2] D.Testa et al., PoP **6** (1999), 3489; and D.Testa et al., PoP **6** (1999), 3498. [3] F.Rimini et al., NF **39** (1999), 1591. [4] A.Salmi et al., EPS 2004. [5] D.Ernst et al., PoP **7** (2000), 615. [6] A.Fasoli et al., PoP **7** (2000), 1816. [7] D.Testa et al., NF **41** (2001), 809. [8] A.Jaun et al., PPCF **43** (2001), A207; and A.Fasoli et al., PLA **265** (2000), 288. [9] W.Suttrop et al., PPCF **39** (1997), 2051. [10] D.Testa et al., NF **43** (2003), 724. [11] D.Testa et al., NF **43** (2003), 479. [12] A.Fasoli et al., IAEA-TCM on Energetic Particles, San Diego, USA, 6-8 October 2003; D.Testa et al., 23rd SOFT, Venice, Italy, 20-24 September 2004.